

Supporting Information

Rossig et al. 10.1073/pnas.1319648110

SI Materials and Methods

Athp20 and Athp30 Mutant Characterization and Analysis of the Athp30/30-2 RNAi Lines. *Athp20;1* and *Athp20;2* (SALK_020671 and SALK_125640) as well as *Athp30;2* and *Athp30;3* (SALK_112126 and SALK_046194) mutant seeds were obtained from the Salk Institute Genomic Analysis Laboratory collection (1). Identification of homozygous mutant plants was performed by PCR-based techniques (2), using appropriate primer combinations (Table S3). For the construction of inverted repeats that give rise to double-stranded RNA and induce the directed degradation of mRNA, published protocols were used (3, 4). Adequate constructs with a hairpin-loop forming intron (PDK, pyruvate orthophosphate dikinase) between sense and anti-sense gene fragments were created with the help of the vector pHannibal (5). The gene fragments were synthesized by PCR (2) and appropriate primers (Table S3), with added restriction sites defining the final orientation (sense/antisense) after cloning.

1. Alonso JM, et al. (2003) Genome-wide insertional mutagenesis of *Arabidopsis thaliana*. *Science* 301(5633):653–657.
2. Innis MA, Gelfand DH, Sninsky JJ, White TJ (1990) *PCR Protocols* (Academic, San Diego, CA).
3. Ruiz-Ferrer V, Voinnet O (2009) Roles of plant small RNAs in biotic stress responses. *Annu Rev Plant Biol* 60:485–510.
4. Kovács-Bogdán E, Soll J, Böltner B (2010) Protein import into chloroplasts: The Tic complex and its regulation. *Biochim Biophys Acta* 1803(6):740–747.
5. Wesley SV, et al. (2001) Construct design for efficient, effective and high-throughput gene silencing in plants. *Plant J* 27(6):581–590.
6. Yin Y, Chory Y, Baulcombe D (2005) RNAi in transgenic plants. *Curr Protoc Mol Biol*, 10.1002/0471142727.mb2606s.
7. Jeanmougin F, Thompson JD, Gouy M, Higgins DG, Gibson TJ (1998) Multiple sequence alignment with Clustal X. *Trends Biochem Sci* 23(10):403–405.
8. Page RDM (1996) TreeView: An application to display phylogenetic trees on personal computers. *Comput Appl Biosci* 12(4):357–358.
9. Edgar RC (2004) MUSCLE: A multiple sequence alignment method with reduced time and space complexity. *BMC Bioinformatics* 5:113.
10. Hofmann K, Stoffel W (1993) TMbase – a database of membrane spanning protein segments. *Biol Chem Hoppe-Seyler* 374:166.
11. Clough SJ, Bent AF (1998) Floral dip: A simplified method for Agrobacterium-mediated transformation of *Arabidopsis thaliana*. *Plant J* 16(6):735–743.

The generated construct was transferred into the binary vector pArt27 (6).

Bioinformatics Tools. Phylogenetic trees were constructed using the sequences outlined in Tables S1 and S2 and the Clustal-X/Treeview, as well as MUSCLE and TMbase programs (7–10).

In Plant Localization of HP20 and HP30. Transformation of *Athp20;1* and *Athp20;2* mutants with DNAs encoding chloroplast-envelope quinone-oxidoreductase homolog (ceQORH)-GFP fusion proteins was performed using appropriate GATEWAY clones (Table S3) and the floral dip method (11). Confocal laser scanning microscopy was carried out with a Leica TCS SP5 microscope with argon laser excitation at 488 nm (GFP) and 561 nm (RFP). GFP, RFP, and chlorophyll were detected at emission wavelengths of 510–525 nm, 575–605 nm, and 650–750 nm, respectively. Leica confocal software LAS AF and Adobe Photoshop 7 (Adobe Systems) were used for image acquisition and processing.

A. Peptides HP20

Peptide 1: AANDSSNAIDIDGNLSDSDSNLNNTDGEATNDSSKALVTIPAPAVCLRFAGDAAGGAVM
 Peptide 2: ALVTIPAPAVCLRFAGDAAGGAVMGSIFGYGSCLF
 Peptide 3: TALAHSVSLRHQTGLFQDH
 Peptide 4: HQTGLFQDH

HP20 1	<u>MAANDSSNAIDIDGNLSDSDSNLNNTDGEATNDSSKALVTIPAPAVCLRFAGDAAGGAV</u> 60
	MAA +SSNAI++D +LDSDS N D ++ TD+DSS + IPAPAVCL RFAGDA GA
HP22 1	<u>MAAENSSNAINVDTSDLSDSKPNRDANDMTDHDSSSKALVIPAPAVCLVRFAGDAASGAF</u> 60
HP20 61	<u>MGSIFGYGSGLFKKKGFKGSFADAGQSAKTFAVLSGVHSLVVCLLKQIRGKDDAINVGVA</u> 120
	MGS+FGYGSGLFKKKGFKGSF DAGQSAKTFAVLSGVHSLVVCLLKQIRGKDDAINVGVA
HP22 61	<u>MGSVFGYGSGLFKKKGFKGSFVDAGQSAKTFAVLSGVHSLVVCLLKQIRGKDDAINVGVA</u> 120
HP20 121	<u>GCCTGLALSFPGAPQALLQSCLTFGAFSFILEGLNKRQTALAHVSLSRHTGLFQDH</u> 180
	GCCTGLALSFPGAPQA+LQSCLTFGAFSFILEGLNKRQTALAHVS R QT +
HP22 121	<u>GCCTGLALSFPGAPQAMLQSCLTFGAFSFILEGLNKRQTALAHVSFRQQT---RSPQHD</u> 177
HP20 181	LP-LSLALPIPEEIKGAFSSFCCKSLAKPRKF 210
	LP LSLA+PI +EIKGAFSSFC SL KP+K
HP22 178	<u>LPILLSLAIPHIDEIKGAFSSFCNSLTKPKKL</u> 208

B. Peptides HP30 and HP30-2**Peptides HP30**

Peptide 1: SSGEMMA MASLFNDQQN PIQQFQVK
 Peptide 2: EVETNFKFTWLSK
 Peptide 3: QSIPVEAAVVSTMSGVQGAFIGGLMGTLSPEMPQAGVDPQAIASMK

Peptides HP30-2:

Peptide 4	LPVEAAVVTAMGGVQGAFIGGLMGTLSPEMPQAGIDPQAMASLK
Peptide 5:	EDLES AVVAFGSGVAYSLVSAGLQQPMNAITTAAGFAVFQGVFFK
HP30 3	VGGGGEGDQKRSSGEMMAMASLFNDQQNP <u>IQQFQVKFKEVETNFKFTWLSKQSI</u> PVEAAVV 62
+G GEGD+KR E MA+ SL DQQNP <u>IQQFQVKFKE+ET FK+WLSKQ</u> +PVEAAVV	
30-2 1	<u>MGKDGEGDKKR---ETMAVMSLMDQQNP<u>IQQFQVKFKEIETGFKSWLSKQKL</u>PVEAAVV</u> 57
HP30 63	<u>STMSGVQGAFIGGLMGTLSPEMPQAGVDPQAIASMKQAAQLVGGPWVQARNFAAITGVNA</u> 122
+ M GVQGAFIGGLMGTLSPEMPQAG+DPQA+AS+KQ QALVGGP VQARNFAAITGVNA	
30-2 58	<u>TAMGGVQGAFIGGLMGTLSPEMPQAGIDPQAMASLKQTLVGGPLVQARNFAAITGVNA</u> 117
HP30 123	GIA SVMKIRKGKEDIESAVVAALGSGFAYSLSVQGLQQPMNAITTAAGFAVFQGVFFKL 182
GIA VMKIRKGKED+ESAVVA GSG AYSLVS GLQQPMNAITTAAGFAVFQGVFFKL	
30-2 118	<u>GIACVMKIRKGKEDLESAVVAAFGSGVAYSLVSAGLQQPMNAITTAAGFAVFQGVFFKL</u> 177
HP30 183	GERFSKPSTEDPFFTRGRGTMVLVKGLEKYEKNFKKGLTDPTLPLLTDSALKDANIPPGP 242
GERFSKPS EDP++TRGR+ML+KLGLEKYEKNFKKGLL DPTLPLLTDSAL+D +IPPGP	
30-2 178	GERFSKPSVEDPYYTRGRSMLLKGLEKYEKNFKKGLADPTLPLLTDSALRDVSIPPGP 237
HP20 243	RLMILDHIQRDPEIKGKR 260
RL+ILDHIQRDPE+KGKR	
30-2 238	RLLILDHIQRDPELGKR 255

Fig. S1. (A) Cyanogen bromide-derived (overlined) and endoproteinase Lys C-derived (underlined) peptides of CLP1 obtained in vitro and amino acid sequence alignment with HP20 (At4g26670) and HP22 (At5g55510). (B) As in A, but showing tryptic peptides (underlined) obtained for CLP2 (Fig. 1) and their alignments with HP30 (At3g49560) and HP30-2 (At5g24650).

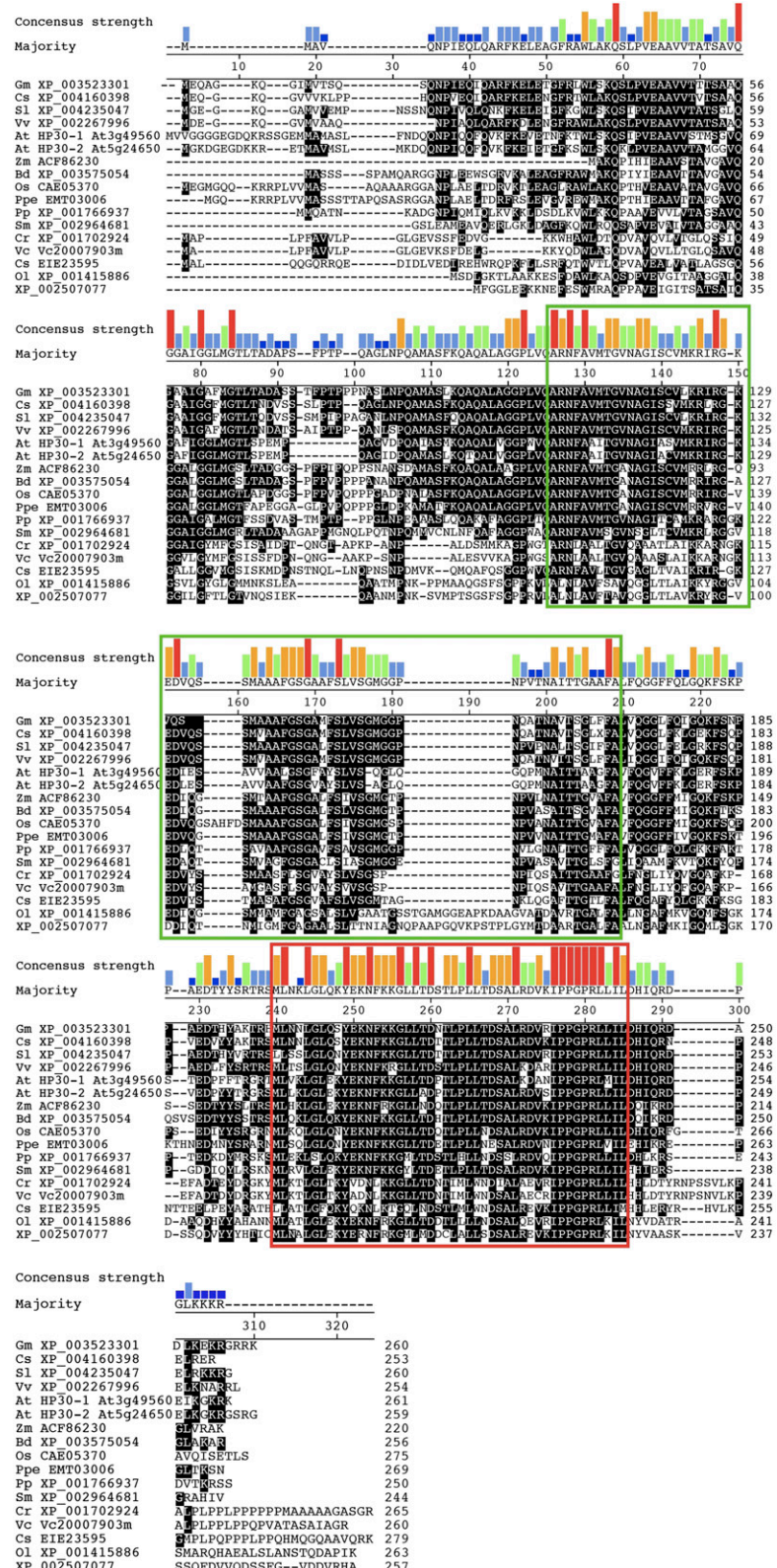


Fig. S2. Multiple sequence alignment of HP-30-like proteins from 17 plant and algal species. The proteins listed in Table S3 were aligned using the CLUSTALW algorithm with default gap opening and extension penalties. The region defining the translocon of the inner mitochondrial membrane (TIM) domain is outlined by a green box. The predicted sterile alpha motif (SAM) domain unique to the HP30-like plant preprotein and amino acid transporter (PRAT) subfamily is outlined by the red box. The consensus motif in Fig. 2C is derived from the consensus sequence in this region (red bars).

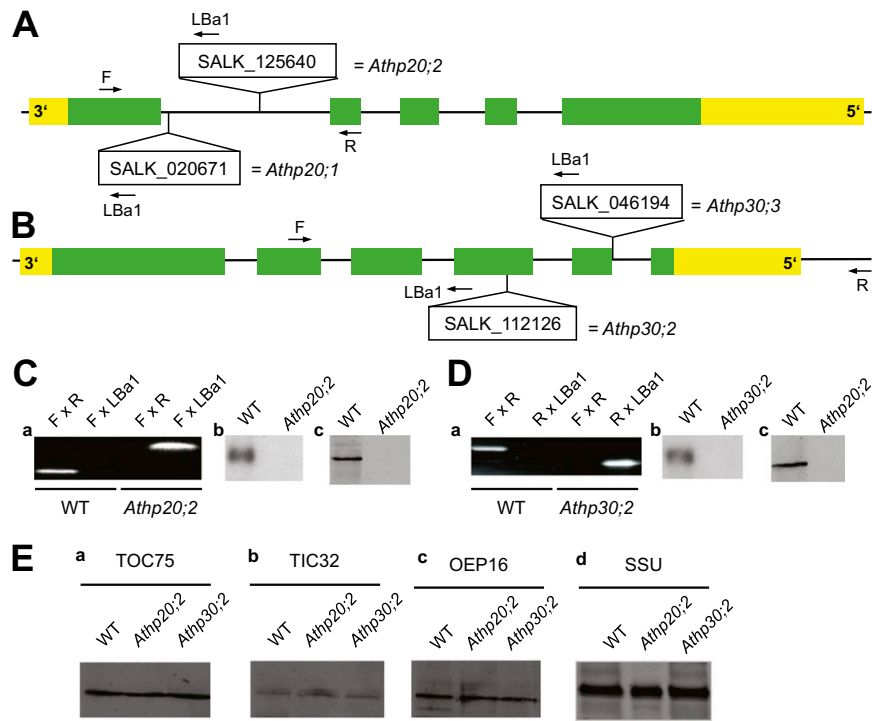


Fig. S3. Identification and characterization of knockout mutants for HP20 and HP30. (A and B) Gene structures, comprising introns and exons, and positions of transfer-DNA (T-DNA) insertions of the respective knockout mutants used in this study. Primers used for genotyping are indicated in Table S1 and highlighted with arrows. (C and D) PCR (a), Northern (b), and Western (c) analyses for *Athp20;2* (C) and *Athp30;2* (D) plants. In b and c, WT controls were included. (E) Protein levels of TOC75 (a), TIC32 (b), OEP16 (c), and the small subunit of ribulose-1,5-bisphosphate carboxylase/oxygenase (SSU) in WT vs. *Athp20;2* and *Athp30;2* plants.

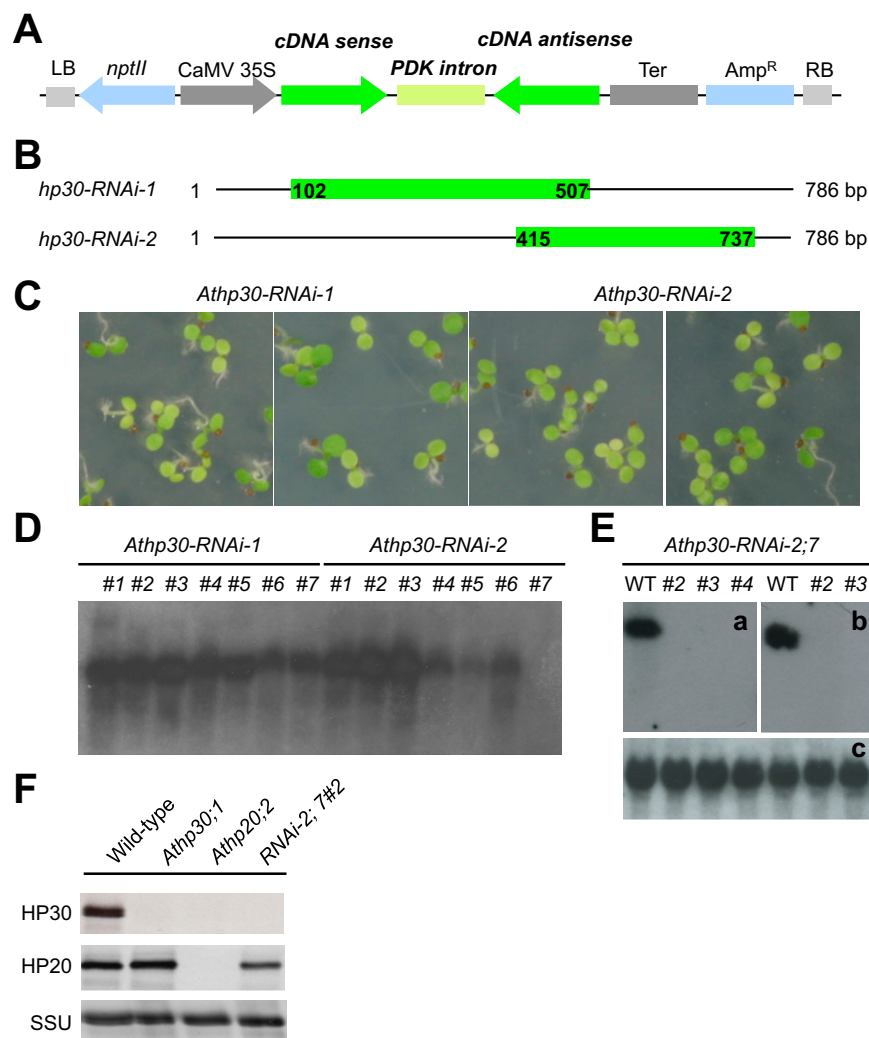


Fig. S4. Creation and characterization of *RNAi* plants lacking HP30 and HP20-2. (A) *RNAi* constructs in the binary vector pArt27 containing the *RNAi* inducing-relevant components between left (LB) and right border (RB). (B) Presentation of the mRNA sequences of *HP20* and *HP30* (green parts) that were selected, in sense direction. Amp^R, ampicillin resistance gene for bacterial selection; CaMV 35S, 35S cauliflower mosaic virus promotor; *nptII*, kanamycin resistance gene (plant selection marker); PDK, pyruvate orthophosphate dikinase; Ter, Terminator. (C) Phenotypes of *Athp30-RNAi-1* and *Athp30-RNAi-2* seedlings after growth for 5 d in 16 h light/8 h dark cycles at 60 $\mu\text{E m}^{-2} \text{s}^{-1}$. (D) Northern blot analysis of HP30 transcripts in the offspring of the different *Athp30-RNAi-1* and *Athp30-RNAi-2* plants. (E) As in D, but showing HP30 (a) and HP30-2 (b) transcript levels in the final mutant plants determined with gene-specific probes (Table S1). For comparison, a replicate blot was probed with an HP20-specific probe (c). (F) Western blot analysis to confirm the absence of expression of HP30 in the final *RNAi-2;7#2* and *RNAi-2;7#3* plants.

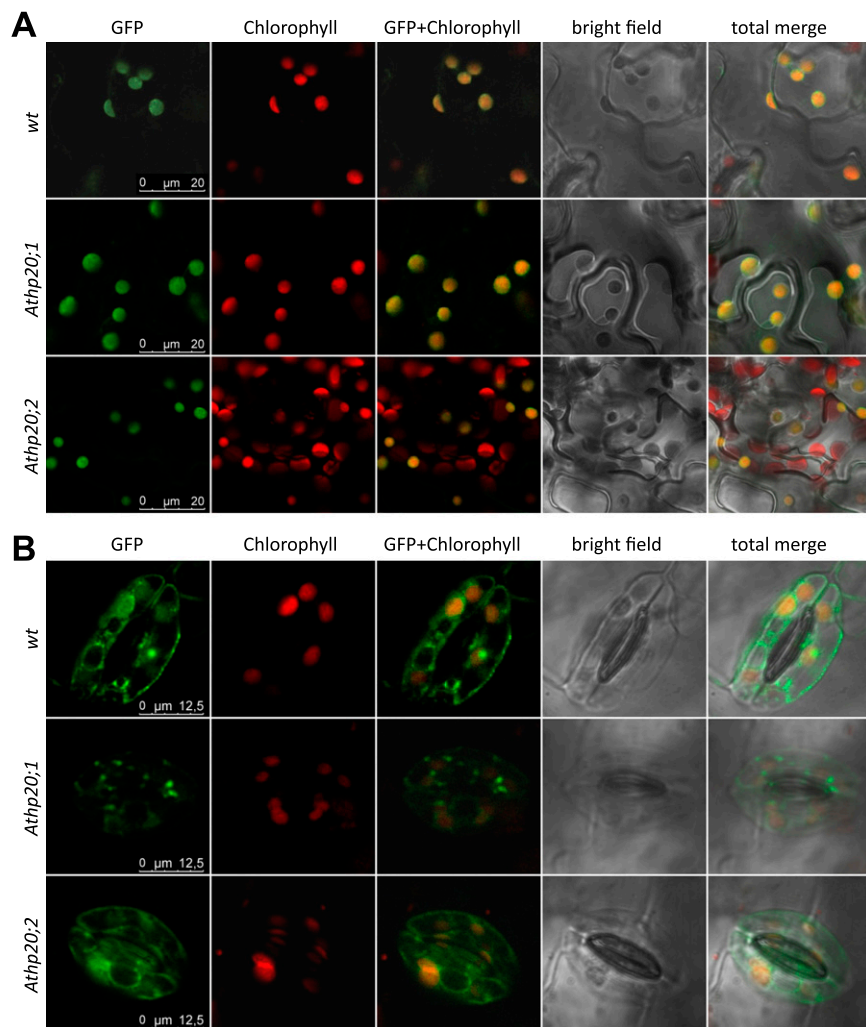


Fig. S5. *In planta* import of ceQORH-GFP in mesophyll cells (*A*) and guard cells (*B*) of plants of the T₂ generation of stably transformed *Arabidopsis thaliana* WT and mutants *Athp20;1* and *Athp20;2*. Fluorescence signals of GFP (green) and chlorophyll (red) were collected simultaneously by confocal laser scanning microscopy. In addition, bright-field images are shown before and after merging the fluorescence signals. Size markers are indicated (bars).

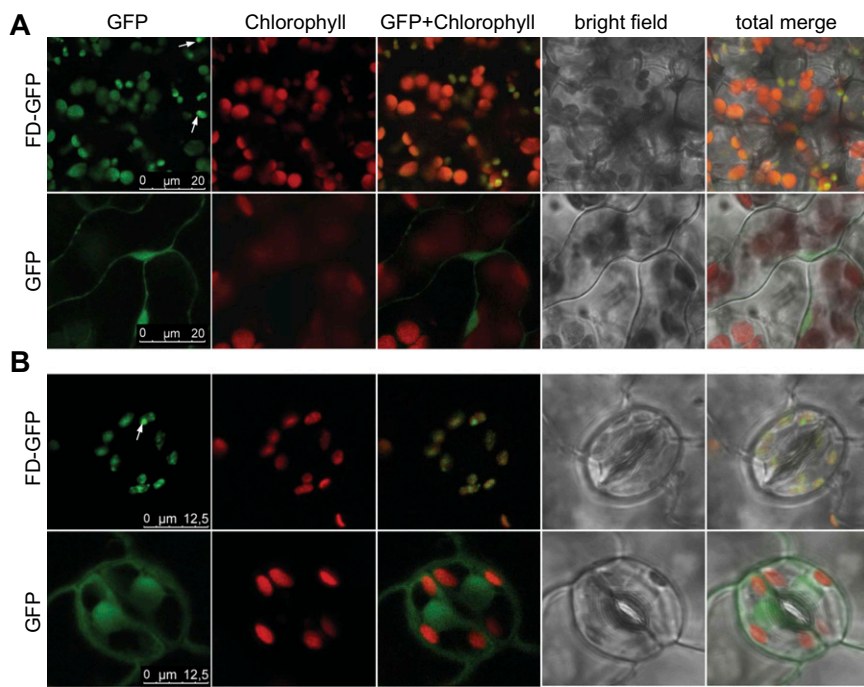


Fig. S6. Subcellular localization of FD-GFP and GFP in mesophyll cells (*A*) and guard cells (*B*) of plants of the *T*₂ generation of stably transformed *A. thaliana* wild-type plants. Fluorescence signals of GFP (green) and chlorophyll (red) were collected simultaneously by confocal laser scanning microscopy. White arrows mark punctual accumulations of GFP fluorescence.

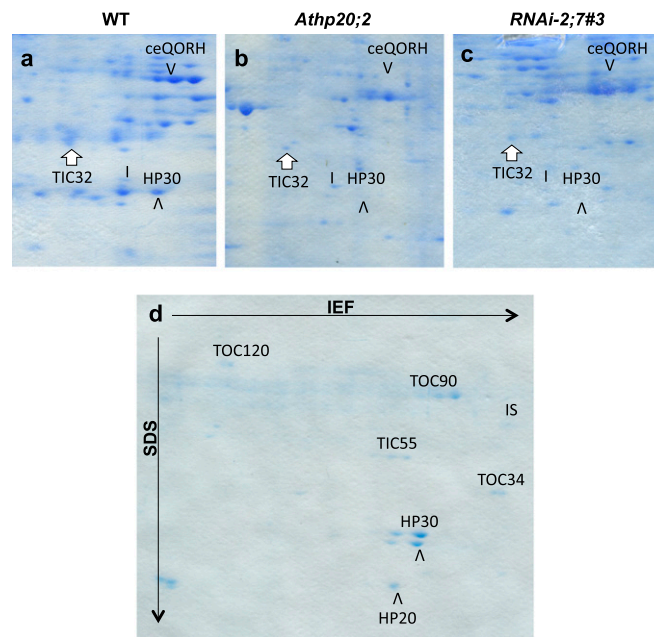


Fig. S7. 2D patterns of basic inner plastid envelope membrane proteins in wild-type (*A*), *Athp20;2* (*B*), and *RNAi-2;7#3* (*C*) chloroplasts. (*D*) A representative 2D pattern of intermediate-associated proteins isolated with ceQORH, used for comparison. The arrowhead and white arrow highlight the positions of ceQORH and TIC32, whereas the vertical bar indicates a protein the abundance of which was similar in all samples.

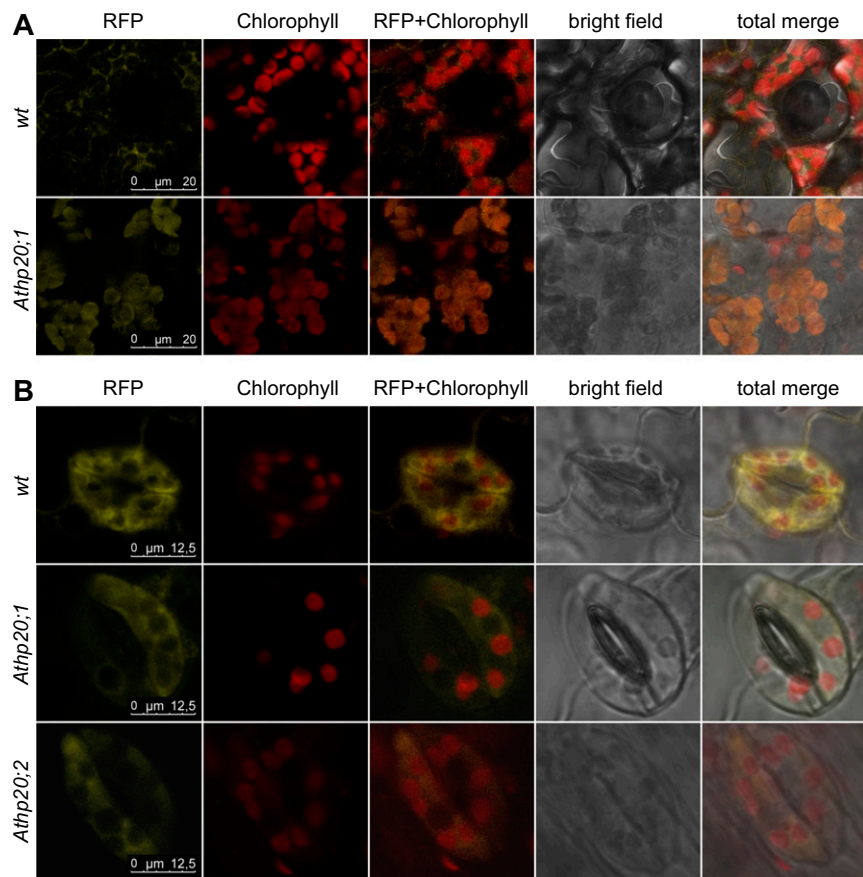


Fig. S8. *In planta* import of TIC32-RFP in mesophyll cells (*A*) and guard cells (*B*) of plants of the T₂ generation of stably transformed *A. thaliana* WT and *Athp20;1* and *Athp20;2* mutants. Fluorescence signals of RFP (yellow) and chlorophyll (red) were collected simultaneously by confocal laser scanning microscopy.

Table S1. List of sequence sources used in Fig. 2

Protein Name	Species	Gene ID or gene model*	GenBank protein ID	TIM domain region
Cr HP30-like	<i>Chlamydomonas reinhardtii</i>	Cre03.g183100.t1*	XP_001702924	91–150
Vc HP30-like	<i>Volvox carteri f. nagariensis</i>	Vocar20007903m*	XP_002946728	89–144
OI HP30-like	<i>Ostreococcus lucimarinus</i> CCE9901	Chr_1:642,207–643,165	XP_001415886	80–135
At HP30-1	<i>Arabidopsis thaliana</i>	At3g49560	ABD64055	111–166
At HP30-2	<i>Arabidopsis thaliana</i>	At5g24650	ABD64056	106–161
At HP20	<i>Arabidopsis thaliana</i>	At4g26670	ABD64059	88–142
At HP22	<i>Arabidopsis thaliana</i>	At5g55510	ABD64060	88–142
Cr HP20/22-like	<i>Chlamydomonas reinhardtii</i>	Cre01.g050400.t2.1*	XP_001689761	103–157
Vc HP20/22-like	<i>Volvox carteri f. nagariensis</i>	Vocar20009762m*	None	97–151
At TIM17-1	<i>Arabidopsis thaliana</i>	At1g20350	AAO63303	63–117
At TIM17-2	<i>Arabidopsis thaliana</i>	At2g37410	NP_973621	63–117
At TIM17-3	<i>Arabidopsis thaliana</i>	At5g11690	NP_196730	63–117
OI TIM17-like	<i>Ostreococcus lucimarinus</i> CCE9901	Chr_1:280,962–281,369	XP_001415788	63–117
Cr TIM17-like	<i>Chlamydomonas reinhardtii</i>	Cre10.g452650.t1.2*	XP_001698342	72–126
Vc TIM17-like	<i>Volvox carteri f. nagariensis</i>	Vocar20010628m*	XP_002957341	71–126
ScTIM17	<i>Saccharomyces cerevisiae</i>	YJL143W	AAS56178	62–116
At OEP16-3	<i>Arabidopsis thaliana</i>	At2g42210	ABD48955	66–122
OI TIM22-like1	<i>Ostreococcus lucimarinus</i> CCE9901	Chr_1:823,163–823,642	XP_001415610	65–120
At3g25120	<i>Arabidopsis thaliana</i>	At3g25120	NP_566759	65–122
Sc TIM22	<i>Saccharomyces cerevisiae</i>	YDL217C	AAS56497	126–180
Cr TIM22-like	<i>Chlamydomonas reinhardtii</i>	XP_001689511	XP_001689511	121–175
Vc TIM22-like	<i>Volvox carteri f. nagariensis</i>	Vocar20010161m*	XP_002952140	122–176
OI TIM22-like	<i>Ostreococcus lucimarinus</i> CCE9901	Chr_5:355,576–356,178	XP_001417996	130–184
At TIM22-1	<i>Arabidopsis thaliana</i>	At1g18320	ABD64057	102–156
At TIM22-2	<i>Arabidopsis thaliana</i>	At3g10110	ABD64057	102–156
At OEP16-1	<i>Arabidopsis thaliana</i>	At2g28900	ABD48954	74–130
At OEP16-2	<i>Arabidopsis thaliana</i>	At4g16160	NP_849394	103–158
Ps OEP16	<i>Pisum sativum</i>	none	Q41050	74–128
At OEP16-4	<i>Arabidopsis thaliana</i>	At3g26880	NP_001030919	60–114
At TIM23-1	<i>Arabidopsis thaliana</i>	At1g17530	NP_564028	111–165
At TIM23-2	<i>Arabidopsis thaliana</i>	At1g72750	NP_177419	112–166
At TIM23-3	<i>Arabidopsis thaliana</i>	At3g04800	ABF83637	111–166
Sc TIM23	<i>Saccharomyces cerevisiae</i>	YNR017W	CAA96296	149–203
Cr g14885.t	<i>Chlamydomonas reinhardtii</i>	g14885.t1*	XP_001689829	101–156
Vc Vocar20008538m	<i>Volvox carteri f. nagariensis</i>	Vocar20008538m*	XP_002946650	101–156

*Gene model identification numbers refer to www.phytozome.net.**Table S2.** List of sequence sources used in Fig. S2

Protein name	Species	Gene ID or gene model*	GenBank protein ID
Cr HP30-like	<i>Chlamydomonas reinhardtii</i>	Cre03.g183100.t1*	XP_001702924
Vc HP30-like	<i>Volvox carteri f. nagariensis</i>	Vocar20007903m*	XP_002946728
OI HP30-like	<i>Ostreococcus lucimarinus</i> CCE9901	Chr_1:642,207–643,165	XP_001415886
At HP30-1	<i>Arabidopsis thaliana</i>	At3g49560	ABD64055
At HP30-2	<i>Arabidopsis thaliana</i>	At5g24650	ABD64056
Zm ACF86230	<i>Zea mays</i>		ACF86230
Os CAE05370	<i>Oryza sativa Japonica</i>		CAE05370
Cs EIE23595	<i>Coccomyxa subellipsoidea</i>		EIE23595
Vv XP_002267996	<i>Vitis vinifera</i>		XP_002267996
Msp XP_002507077	<i>Micromonas sp. RCC299</i>		XP_002507077
Sm XP_002964681	<i>Selaginella moellendorffii</i>		XP_002964681
Grm XP_003523301	<i>Glycine max</i>		XP_003523301
SI XP_004235047	<i>Solanum lycopersicum</i>		XP_004235047
Pp XP_001766937	<i>Physcomitrella patens</i> subsp. <i>patens</i>		XP_001766937
Ppe EMT03006	<i>Prunus persica</i>		EMT03006
Bd XP_003575054	<i>Brachypodium distachyon</i>		XP_003575054
Cs XP_004160398	<i>Cucumis sativus</i>		XP_004160398

*Gene model identification numbers refer to www.phytozome.net.

Table S3. List of oligonucleotides and their application

Notation	Sequence (5'-3')	Application
Prot HP20F1	attB1 ^a + GCGGCGAACGATTCTCA	
Prot HP20R1	attB2 ^b + <u>TTAGAACTTCCTGGTTTAGC</u>	Cloning (without start codon) into pDEST17 for heterologous expression of N-terminally His-tagged proteins
Prot HP30F1	attB1 + GTGGTAGGCAGGAGGA	
Prot HP30R1	attB2 + <u>CTACTTCTGTTGCCCTTATCTC</u>	
At5g5551-FW1	attB1 + GCGGCCGAGAATTCTCAAAC	
At5g5551-RW1	attB2 + <u>TCAACGAGCATGAGGAAATT</u>	
At5g24650-FW1	attB1 + GGGAAAGACGGAGAAGGAGAC	
At5g24650-RW1	attB2 + <u>TCAACCACGACTTCCCCGCTT</u>	
Hp20GFPF1	attB1 + <u>ATGGCGGCAGAACGATTCTCA</u>	Cloning (without stop codon) into pK7FWG2 or pB7RWG2 for in vivo localization via C-terminally tagged GFP/RFP
Hp20GFPF1	attB2 + AAGCTTCTGGTTAGCTAA	
Hp30GFPF1	attB1 + <u>ATGGTGGTAGGCAGGAGGAGAA</u>	
Hp30GFPF1	attB2 + CTTCGTTGCCCTTATCTC	
Tic32RFPF1	attB1 + <u>ATGTGGTTTTGGATCG</u>	
Tic32RFPR1	attB2 + AGAACTGTTCTCTGA	
ceqorhFWatt	attB1 + <u>ATGGCTGAAAACATGACGCTC</u>	
ceqorhRWatt	attB2 + TGGCTGACAATGATCTCCAGTA	
FdGFP	attB1 + <u>ATGGCTTCTACACTCTTAC</u>	
FdGFPF1	attB2 + AGCAGTAAGTCCCTCCCTT	
LBa1	TGGTTCACGTTGGGCATCG	Genotyping of <i>A. thaliana</i> T-DNA insertion lines
HP20PF	CTATTGACATCGACGGGAAT	
HP20PR	TGCAAATGATCCTTGAAAGC	
HP30GT1	AAGCGGATTAGAGGCAAAGAG	
HP30GT2	GATTGGCCAATTGTATGAACC	
KanF2	CTATGACTGGGCACAAACAGAC	Production of digoxigenin-labeled probes for specific DNA or RNA detection on southern and Northern blots
KanR2	GAAGGGCATAGAAGGGGATG	
LB GT1	ACTTAATAACACATTGCGGACG	
LB GT2	CTTAATCGCTTGCAGCACATC	
hp20-F1	GTGACGAAGCGACCGATAATG	
hp20-R1	ATTCTTCAGGGATCGGGAGAG	
hp30-F1	GCGATGGCGAGTTATTCAACG	
hp30-R1	CCTTATCTCGGGTCCCTCT	
POR-fwd	attB1 + <u>ATGGCCCTCAAGCTGCTTCT</u>	Detection of transcripts by RT-PCR and subsequent cloning
POR-rev	attB2 + <u>TTTAGGCCAACCTACGAGC</u>	
PORA-utr-fwd	attB1 + TAACATTACATTACACTCT	
PORA-utr-rev	attB2 + TGTTTCTGTTAACACTTAA	
FLU-fwd	attB1 + <u>ATGTGGCAGGAAATTGGGAGG</u>	
FLU-rev	attB2 + <u>TCAGTCAGTCTAACCGAGC</u>	
HP20RNAiF3	GAC <u>GGATCCCTCGAG</u> TAATGATTCTCGAAGGCATT	Production of RNAi constructs in pHannibal (forward primers with <i>Bam</i> HI and <i>Xba</i> I; reverse primers with <i>Kpn</i> I and <i>Hind</i> III restriction sites)
HP20RNAiF4	GAC <u>GGATCCCTCGAG</u> TGCCCTCTGAAGCAAATCGA	
HP20RNAiR3	CTG <u>AAGCTTGTACCA</u> AACGTGAGACAACACTGTAG	
HP20RNAiR4	CTG <u>AAGCTTGTACCTTGATTTCTCAGGGATCGG</u>	
HP30RNAiF3	GAC <u>GGATCCCTCGAG</u> TTTCAGGTTAAATTCAAAGA	
HP30RNAiF4	GAC <u>GGATCCCTCGAG</u> TCTGCAGTGGGGCAGCGTTA	
HP30RNAiR3	CTG <u>AAGCTTGTACCA</u> AGCAGTAGTGTATTGCATTAT	
HP30RNAiR4	CTG <u>AAGCTTGTACCA</u> ATATAAGTCTGGCCCTGGT	
RNAiPDKF1	TGACAAGTGTGTAAAGACG	Identification of transformed <i>A. thaliana</i> plants by amplification of the PDK intron in RNAi lines, the <i>gfp/rfp</i> sequences and the connection between cDNA and fluorescence tag
RNAiPDKR1	AATGATAGATCTTGCCTTG	
FdGFPF2	TCTCGGGCAGAGTGACTGC	
HP20GFPF2	CTCAGGCTTGTGGGTGGT	
HP30GFPF2	AGATGCAGGGCAGTGTCTAA	
Tic32RFPF2	CGGTTCTGTATCCAGAACGGAGT	
QORGFPF2	AACCGCTCTCAAGCTCTTAC	
egfp1	ATGGTGAGCAAGGGCGAG	
egfp2	GGTGCCTCTGGACGTA	
rfp1	CGACTACTTGAAGCTGTCTCT	
rfp2	CTCGTACTGTTCCACGATG	
rfp3	AAGTTCATACGCGCTCCACT	
^a attB1	GGGGACAAGTTGTACAAAAAAGCAGGCTCC	
^b attB2	GGGGACCACTTGTACAAGAAAGCTGGGTC	

Restriction sites are highlighted in color. Start and stop codons are underlined. Synthesis was carried out by Sigma-Genosys, MWG Biotech AG, and Invitrogen.